Available online at www.eccomasproceedia.org
Eccomas Proceedia SMART (2023) 1574-1585

ECCOMAS
Proceedia

X ECCOMAS Thematic Conference on Smart Structures and Materials
SMART 2023
D.A. Saravanos, A. Benjeddou, N. Chrysochoidis and T. Theodosiou (Eds)

NONLINEAR BEHAVIOUR AND HOMOGENIZATION OF METAPLATES

David Faraci and Claudia Comi

Department of Civil and Environmental Engineering
Politecnico di Milano
Piazza Leonardo da Vinci 32, 20133 Milan, Italy
e-mail: david.faraci@polimi.it, claudia.comi@polimi.it

Abstract. Large deflections in thin plates introduce a nonlinear membrane-flexural coupling which significantly modifies the plate behaviour under transversal and in-plane loading. This effect is often important when considering metamaterial plates with periodically distributed heterogeneities or holes. In this work, we employ the asymptotic homogenization technique to study the effective nonlinear behaviour of periodic Föppl-von Kármán plates in the static regime. Then, we validate the method by simulating the nonlinear response of the perforated plate (backplate) which is present in a micro-electro-mechanical microphone to limit the displacements of the vibrating membrane.

Key words: Metaplates, nonlinear plates, periodic plates, asymptotic homogenization

1 INTRODUCTION

When the out-of-plane deflection of a plate is sufficiently large with respect to its thickness, non-negligible membrane deformations and membrane forces can arise. These latter can play a significant role in the transversal equilibrium of thin plates. The simplest theory that accounts for the coupling between the membranal and flexural behaviour is the non-linear model of Föppl and von Kármán [1] where the equilibrium of thin plates is studied under the hypothesis of small strains and moderately large displacements.

The nonlinear membrane-flexural coupling is often important when considering periodically perforated plates since the presence of holes increases the compliance and hence the holed plate undergoes larger displacements than the homogeneous one. The numerical simulation of such periodic structure is expensive from the computational point of view, not only due to the fine mesh required to discretise the complex geometry, but also due to the nonlinearity of the analysis.

Asymptotic homogenization is a mathematical technique that allows studying the effective behaviour of media with periodic heterogeneities, which can be voids or different materials [2]. For fully linear problems, the method allows to obtain explicit expressions of the homogenized properties of periodic solids [3, 4, 5] and plates [6, 7] both in the static and dynamic regime.

Peer-review under responsibility of the organizing committee of SMART 2023.
doi: 10.7712/150123.9929.444134

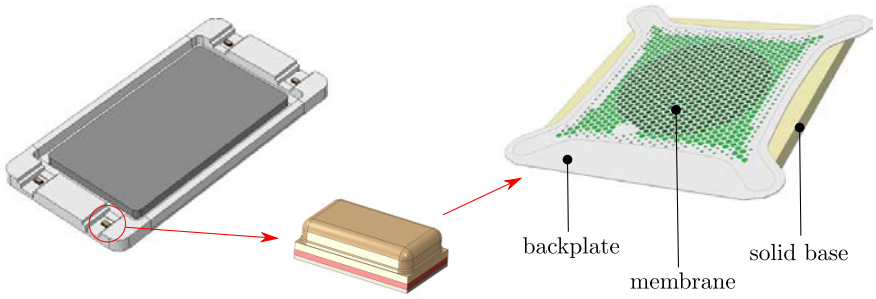

Figure 1: Jig geometry (left) with a close-up view of the capsule (middle) containing the MEMS microphone; (c) model of the structural part: backplate, membrane and solid base.

As discussed in [8], the two-scale asymptotic homogenization can be extended to the particular nonlinear problem described by the Föppl-von Kármán model. As the size of the unit cell tends to zero, the homogenization approach allows to study the global buckling and the post-bifurcation regime of thin plates [9], with a significant advantage in terms of computational time.

In this work, we summarize the asymptotic homogenization of Föppl-von Kármán plates in the static regime. Then, we validate the method by analyzing the nonlinear behaviour of a perforated plate with reference to a specific application for a Micro-Electro-Mechanical-System (MEMS) microphone.

Figure 1 shows, on the right, the mechanical part of the MEMS microphone which is composed of a thin silicon membrane (in green) whose transversal displacement is limited by a thin silicon-nitride plate (the backplate, in grey). Figure 1 shows also a solid portion of the chamber (in yellow) where the microphone is located. The whole MEMS is packaged in a capsule (middle) which is placed on portable devices, such as smartphones. To assess the reliability of the microphones, drop tests are usually performed on a dummy device, also called *jig*, shown on the left in Figure 1.

Accidental drops may lead to a complete failure of the MEMS microphone, which is caused by the combined effect of

- the air overpressure acting on the microphone components due to the fall, which is provoked by the airflow passing through a narrow duct that connects the MEMS chamber with the exterior environment;
- the relative displacements of the microphone anchors due to the propagation of stress waves generated by the first impact (and subsequent impacts) of the jig against the ground.

As explained in [10], experimental guided free-fall tests are not resolutive for a complete understanding of the physical phenomena. Finite element analyses are thus mandatory to understand under which conditions the MEMS microphone fails.

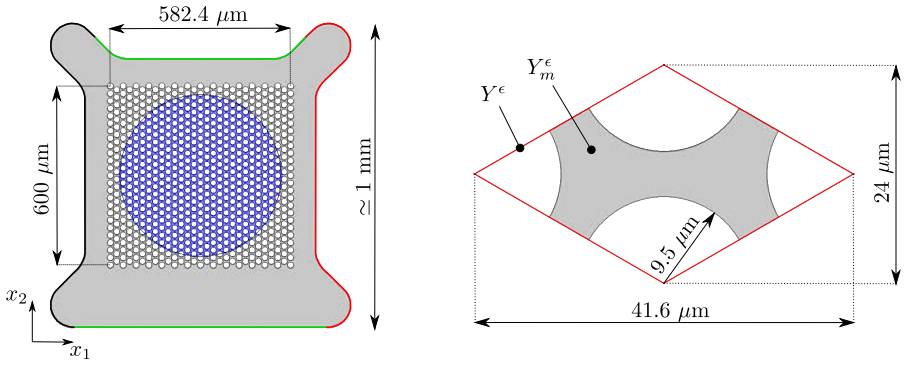

(a) (b)

Figure 2: (a) Simplified geometry of the backplate, loaded on the blue-shaded area, with boundary conditions: black portion is clamped, green portion can only slide horizontally and red portion is inward displaced. (b) Unit cell of the backplate.

In particular, the anchor displacements have been carefully modeled in [11] with special regard for the backplate, which has been shown to exhibit significant nonlinear effect due to the combined membrane (the anchor imposed motion) and transversal loading (air pressure and contact with the membrane). In this framework, asymptotic homogenization could be useful to reduce the computational cost of the many simulations of the MEMS backplate, corresponding to different combinations of imposed displacements and pressure.

2 HOMOGENIZATION OF NONLINEAR THIN PLATES

Let us consider a non-homogeneous plate having mid-surface Ω, as the central portion of the backplate of Figure 2a, which is characterized by the periodic repetition of a unit cell Y^ϵ (see Figure 2b). The plate thickness $h^\epsilon(\mathbf{x})$ and material properties are assumed to vary periodically.

In the hypothesis of scale separation, i.e., when the ratio ϵ between the characteristic sizes of the unit cell and of the macroscopic domain is sufficiently small, the effective behaviour of the periodic plate can be studied through asymptotic homogenization.

Assuming linear-elastic materials and moderately large displacements, the equilibrium of the periodic plate is governed by the set of equations

$$\begin{cases} \nabla \cdot \mathbf{N}^\epsilon + \mathbf{q}^\epsilon = \mathbf{0} \\ \nabla \cdot (\nabla \cdot \mathbf{M}^\epsilon) + \nabla \cdot (\mathbf{N}^\epsilon \cdot \nabla w^\epsilon) + p^\epsilon = 0 \end{cases} \quad \text{in } \Omega. \tag{1}$$

In (1) p^ϵ and $\mathbf{q}^\epsilon$ are, respectively, the transversal and membrane applied loads, and

$$\begin{aligned} \mathbf{N}^\epsilon &= N_{11}^\epsilon \mathbf{e}_1 \otimes \mathbf{e}_1 + N_{22}^\epsilon \mathbf{e}_2 \otimes \mathbf{e}_2 + N_{12}^\epsilon \mathbf{e}_1 \odot \mathbf{e}_2, \\ \mathbf{M}^\epsilon &= M_{11}^\epsilon \mathbf{e}_1 \otimes \mathbf{e}_1 + M_{22}^\epsilon \mathbf{e}_2 \otimes \mathbf{e}_2 + M_{12}^\epsilon \mathbf{e}_1 \odot \mathbf{e}_2. \end{aligned} \quad \text{in } \Omega, \tag{2}$$

where $\mathbf{e}_1$ and $\mathbf{e}_2$ are the unit vectors of the reference frame $x_1 - x_2$. In equation (2), $N_{11}^\epsilon, N_{22}^\epsilon$ and N_{12}^ϵ are the normal and shear membrane forces, while $M_{11}^\epsilon, M_{22}^\epsilon$ and M_{12}^ϵ are the bending

and torsional moments. For elastic plates, the tensors $\mathbf{N}^\epsilon$ and $\mathbf{M}^\epsilon$ can be expressed as functions of the in-plane displacement vector $\mathbf{u}^\epsilon = u_1\mathbf{e}_1 + u_2\mathbf{e}_2$ and of the out-of-plane displacement component w^ϵ through

$$\mathbf{N}^\epsilon = \mathbb{A}^\epsilon : \left(\boldsymbol{\varepsilon}(\mathbf{u}^\epsilon) + \frac{1}{2}\nabla w^\epsilon \otimes \nabla w^\epsilon\right) \quad \text{and} \quad \mathbf{M}^\epsilon = -\mathbb{B}^\epsilon : \nabla \otimes \nabla w^\epsilon \qquad \text{in } \Omega, \tag{3}$$

with $\boldsymbol{\varepsilon}(\mathbf{u}^\epsilon)$ denoting the symmetric part of the displacement gradient $\nabla\mathbf{u}^\epsilon$. In equation (3), $\mathbb{A}^\epsilon$ and $\mathbb{B}^\epsilon$ are the plate membrane and flexural stiffnesses, which can be expressed in terms of the Young's modulus E^ϵ and the Poisson's coefficient ν^ϵ as

$$\mathbb{A}^\epsilon = \mathbb{D}_p^\epsilon h^\epsilon \quad \text{and} \quad \mathbb{B}^\epsilon = \mathbb{D}_p^\epsilon \frac{(h^\epsilon)^3}{12}, \quad \text{with} \quad \mathbb{D}_p^\epsilon = \frac{E^\epsilon}{1-(\nu^\epsilon)^2}\left[(1-\nu^\epsilon)\mathbb{I} + \nu^\epsilon \mathbf{I}\otimes\mathbf{I}\right]. \tag{4}$$

According to the two-scale asymptotic homogenization technique, we introduce the fast variable $\mathbf{y} = \mathbf{x}/\epsilon$ and the re-scaled unit cell $Y = Y^\epsilon/\epsilon$ of the periodic plate. For any field $f(\mathbf{x},\mathbf{y})$ we denote by $\nabla_\mathbf{x} f$ and $\nabla_\mathbf{y} f$ the gradients of f with respect to the slow and fast variables, respectively, so that $\nabla f = \nabla_\mathbf{x} f + \epsilon^{-1}\nabla_\mathbf{y} f$. Similarly, the symmetric part of the displacement gradients with respect to $\mathbf{x}$ and $\mathbf{y}$ are denoted by $\boldsymbol{\varepsilon}_\mathbf{x}$ and $\boldsymbol{\varepsilon}_\mathbf{y}$. The solution of problem (1) is searched assuming the following expansions

$$\begin{aligned} \mathbf{u}^\epsilon(\mathbf{x}) &= \mathbf{u}^0(\mathbf{x},\mathbf{x}/\epsilon) + \epsilon\,\mathbf{u}^1(\mathbf{x},\mathbf{x}/\epsilon) + o(\epsilon) \\ w^\epsilon(\mathbf{x}) &= w^0(\mathbf{x},\mathbf{x}/\epsilon) + \epsilon\,w^1(\mathbf{x},\mathbf{x}/\epsilon) + \epsilon^2 w^2(\mathbf{x},\mathbf{x}/\epsilon) + o(\epsilon^2) \end{aligned} \qquad \text{in } \Omega, \tag{5}$$

where the fields $\mathbf{u}^i(\mathbf{x},\mathbf{y}), w^i(\mathbf{x},\mathbf{y})$ are defined on $\Omega\times Y$ and are $Y-$periodic with respect the second variable. The plate thickness and the material properties are assumed to vary only at the micro-scale, which means

$$h^\epsilon(\mathbf{x}) = h(\mathbf{x}/\epsilon), \quad \mathbb{A}^\epsilon(\mathbf{x}) = \mathbb{A}(\mathbf{x}/\epsilon), \quad \text{and} \quad \mathbb{B}^\epsilon(\mathbf{x}) = \mathbb{B}(\mathbf{x}/\epsilon) \qquad \text{in } \Omega, \tag{6}$$

while the external loadings can also exhibit a variation within the macroscopic domain, i.e.,

$$\mathbf{q}^\epsilon(\mathbf{x}) = \mathbf{q}(\mathbf{x},\mathbf{x}/\epsilon) \quad \text{and} \quad p^\epsilon(\mathbf{x}) = p(\mathbf{x},\mathbf{x}/\epsilon) \quad \text{in } \Omega. \tag{7}$$

All the fields $h(\mathbf{y}), \mathbb{A}(\mathbf{y}), \mathbb{B}(\mathbf{y}), \mathbf{q}(\mathbf{x},\mathbf{y})$ and $p(\mathbf{x},\mathbf{y})$ are defined on $\Omega\times Y$ and are $Y-$periodic with respect the fast variable $\mathbf{y}$.

Replacing (5), (6) and (7) into the governing equations (1), (3) and (4) one obtains a sequence of differential problems to be solved for each order of the parameter ϵ. In particular, it is possible to prove that the fields $\mathbf{u}^0, w^0$ and w^1 are independent of $\mathbf{y}$, namely

$$\mathbf{u}^0(\mathbf{x},\mathbf{y}) = \mathbf{U}^0(\mathbf{x}), \quad w^0(\mathbf{x},\mathbf{y}) = W^0(\mathbf{x}) \quad \text{and} \quad w^1(\mathbf{x},\mathbf{y}) = W^1(\mathbf{x}) \quad \text{in } \Omega\times Y, \tag{8}$$

while the leading terms of the membrane forces and moments are given by

$$\begin{aligned} \mathbf{N}^0(\mathbf{x},\mathbf{y}) &= \mathbb{a}^0(\mathbf{y}) : \left(\boldsymbol{\varepsilon}_\mathbf{x}(\mathbf{U}^0(\mathbf{x})) + \frac{1}{2}\nabla_\mathbf{x} W^0(\mathbf{x})\otimes\nabla_\mathbf{x} W^0(\mathbf{x})\right) \\ \mathbf{M}^0(\mathbf{x},\mathbf{y}) &= -\mathbb{b}^0(\mathbf{y}) : \nabla_\mathbf{x}\otimes\nabla_\mathbf{x} W^0(\mathbf{x}) \end{aligned} \qquad \text{in } \Omega\times Y. \tag{9}$$

For each point $\mathbf{x} \in \Omega$ of the homogenized plate, equation (9) allows to reconstruct the local membrane forces and moments within the re-scaled unit cell Y. Their evaluation is obtained by combining the homogenized displacements $\mathbf{U}^0(\mathbf{x}), W^0(\mathbf{x})$ with the so-called stress localization tensors $\mathbb{a}^0(\mathbf{y})$ and $\mathbb{b}^0(\mathbf{y})$, whose components are given by

$$\begin{aligned} a^0_{ijhk}(\mathbf{y}) &= (\mathbf{e}_i \odot \mathbf{e}_j) : \mathbb{A}(\mathbf{y}) : (\mathbf{e}_h \odot \mathbf{e}_k + \boldsymbol{\varepsilon}_{\mathbf{y}}(\boldsymbol{\alpha}^{hk}(\mathbf{y}))) \\ b^0_{ijhk}(\mathbf{y}) &= (\mathbf{e}_i \odot \mathbf{e}_j) : \mathbb{B}(\mathbf{y}) : (\mathbf{e}_h \odot \mathbf{e}_k - \nabla_{\mathbf{y}} \otimes \nabla_{\mathbf{y}} \beta^{hk}(\mathbf{y})) \end{aligned} \qquad \text{in } Y, \tag{10}$$

for $i, j \in \{1, 2\}$. In equation (10), $\boldsymbol{\alpha}^{ij}(\mathbf{y})$ and $\beta^{ij}(\mathbf{y})$ are the solutions of the following linear-elastic problems

$$\boldsymbol{\alpha}^{ij}(\mathbf{y}) \rightarrow \begin{cases} \nabla_{\mathbf{y}} \cdot [\mathbb{A} : (\boldsymbol{\varepsilon}_{\mathbf{y}}(\boldsymbol{\alpha}^{ij}) + \mathbf{e}_i \odot \mathbf{e}_j)] = \mathbf{0} & \text{in } Y \\ \boldsymbol{\alpha}^{ij} \text{ periodic} & \text{on } \partial Y \\ [\mathbb{A} : (\boldsymbol{\varepsilon}_{\mathbf{y}}(\boldsymbol{\alpha}^{ij}) + \mathbf{e}_i \odot \mathbf{e}_j)] \cdot \mathbf{n} \text{ anti-periodic} & \text{on } \partial Y \end{cases}, \tag{11}$$

$$\beta^{ij}(\mathbf{y}) \rightarrow \begin{cases} \nabla_{\mathbf{y}} \cdot (\nabla_{\mathbf{y}} \cdot \mathbf{M}^{ij}) = 0 & \text{in } Y \\ \beta^{ij},\ \mathbf{n} \cdot \mathbf{M}^{ij} \cdot \mathbf{n} \text{ periodic} & \text{on } \partial Y \\ \nabla_{\mathbf{y}} \beta^{ij} \cdot \mathbf{n},\ (\nabla_{\mathbf{y}} \cdot \mathbf{M}^{ij}) \cdot \mathbf{n} + \nabla_{\mathbf{y}} (\mathbf{t} \cdot \mathbf{M}^{ij} \cdot \mathbf{n}) \cdot \mathbf{t} \text{ anti-periodic} & \text{on } \partial Y \end{cases}, \tag{12}$$

where $\mathbf{M}^{ij} = \mathbb{B} : (-\nabla_{\mathbf{y}} \otimes \nabla_{\mathbf{y}} \beta^{ij} + \mathbf{e}_i \odot \mathbf{e}_j)$, while $\mathbf{n}$ and $\mathbf{t}$ are the unit normal and tangential vectors of the cell boundary. The function $\boldsymbol{\alpha}^{ij}(\mathbf{y})$ (resp. $\beta^{ij}(\mathbf{y})$) is the in-plane (resp. out-of-plane) displacement field of the plate unit cell Y when it is subject to a uniform membrane eigenstrain (resp. eigencurvature) $\mathbf{e}_i \odot \mathbf{e}_j$ and periodic boundary conditions.

The homogenized equilibrium equations of the nonlinear plate read

$$\begin{cases} \nabla_{\mathbf{x}} \cdot \langle \mathbf{N}^0 \rangle + \langle \mathbf{q} \rangle = \mathbf{0} \\ \nabla_{\mathbf{x}} \cdot (\nabla_{\mathbf{x}} \cdot \langle \mathbf{M}^0 \rangle) + \nabla_{\mathbf{x}} \cdot (\langle \mathbf{N}^0 \rangle \cdot \nabla_{\mathbf{x}} W^0) + \langle p \rangle = 0 \end{cases} \qquad \text{in } \Omega. \tag{13}$$

where we have introduced the average operator over the re-scaled unit cell

$$\langle \diamond \rangle = \frac{1}{|Y|} \int_Y \diamond \, d\mathbf{y}. \tag{14}$$

Through equation (9), the average plate forces and moments can be expressed as

$$\begin{aligned} \langle \mathbf{N}^0 \rangle &= \mathbb{A}^0 : \left(\boldsymbol{\varepsilon}_{\mathbf{x}}(\mathbf{U}^0) + \frac{1}{2} \nabla_{\mathbf{x}} W^0 \otimes \nabla_{\mathbf{x}} W^0 \right) \\ \langle \mathbf{M}^0 \rangle &= -\mathbb{B}^0 : \nabla_{\mathbf{x}} \otimes \nabla_{\mathbf{x}} W^0 \end{aligned} \qquad \text{in } \Omega, \tag{15}$$

where $\mathbb{A}^0 = \langle \mathbb{a}^0 \rangle$ and $\mathbb{B}^0 = \langle \mathbb{b}^0 \rangle$ are the homogenized membrane and bending stiffness of the plate.

As can be seen from (13), the homogenized plate obeys the Föppl-von Kármán theory. In particular, the homogenized stiffnesses $\mathbb{A}^0$ and $\mathbb{B}^0$ of the plate are obtained by the solution of

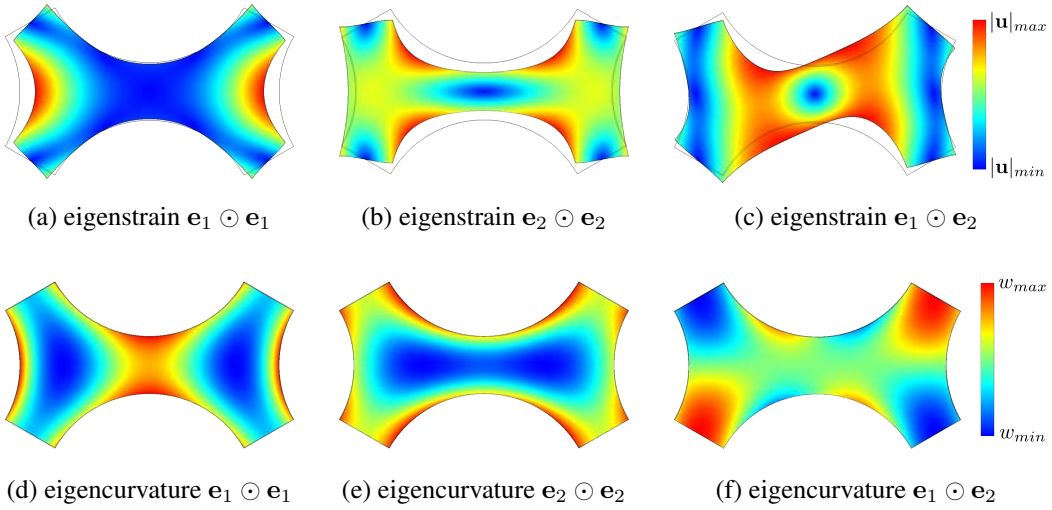

(a) eigenstrain $\mathbf{e}_1 \odot \mathbf{e}_1$ (b) eigenstrain $\mathbf{e}_2 \odot \mathbf{e}_2$ (c) eigenstrain $\mathbf{e}_1 \odot \mathbf{e}_2$

(d) eigencurvature $\mathbf{e}_1 \odot \mathbf{e}_1$ (e) eigencurvature $\mathbf{e}_2 \odot \mathbf{e}_2$ (f) eigencurvature $\mathbf{e}_1 \odot \mathbf{e}_2$

Figure 3: Contours of the displacement magnitude of the solution of the membrane cell problems (a,b,c) and of the out-of-plane displacement of the solution of the flexural cell problems (d,e,f).

linear-elastic cell problems and are therefore independent of the nonlinear behaviour of the plate. This result is due to the particular nonlinearity considered in the Föppl-von Kármán model, and may not remain true when considering different kinds of geometrical or material nonlinearities.

Note that, even if from (4) one has $\mathbb{B} = \mathbb{A}h^2/12$, in general, the homogenized membranal and flexural stiffness of the plate are no more related, i.e., $\mathbb{B}^0 \neq \mathbb{A}^0 h^2/12$.

3 NUMERICAL EXAMPLE

To validate the non-linear homogenization of Föppl-von Kármán plates, we refer to the practical application of MEMS microphones, devices which are commonly used in smartphones.

To this purpose, we consider a simplified geometry of the backplate, shown in Figure 2a. The thickness is assumed uniform and equal to 3 μm, while the constituent material is modeled as isotropic with Young's modulus $E = 169$ GPa and Poisson's ratio $\nu = 0.3$.

3.1 Homogenization of the inner region

The central portion of the backplate, a rectangle of size $582.4\ \mu\text{m} \times 600\ \mu\text{m}$, is periodically perforated by circular holes of radius $R = 9.5\ \mu$m according to a rhomboidal pattern. Figure 2b shows a close-up view of the unit cell Y^ϵ of the periodic region.

To characterize the effective homogenized behaviour of the periodic structure, one has to solve the membrane (11) and flexural (12) cell problems by finite element analysis. Figures 3 a, b and c show the solution of cell problems $\boldsymbol{\alpha}^{11}$, $\boldsymbol{\alpha}^{22}$ and $\boldsymbol{\alpha}^{12}$, associated (respectively) to a uniform horizontal and vertical longitudinal eigenstrain, and to a uniform angular eigenstrain.

In the second row, the solution of the flexural cell problems β^{11}, β^{22} and β^{12} associated to uniform imposed bending (Figure 3 d,e) and torsional (Figure 3 f) eigencurvatures are reported.

On the basis of the solution of the cell problems, the stress localization tensors $\mathbb{a}^0$ and $\mathbb{b}^0$ can be computed through equation (10). Finally, the homogenized membrane and bending stiffnesses $\mathbb{A}^0$ and $\mathbb{B}^0$ of the backplate perforated region are obtained by averaging the tensors $\mathbb{a}^0$ and $\mathbb{b}^0$ over the re-scaled unit cell Y.

3.2 Validation of the homogenized properties

The simplified backplate of Figure 2a is numerically simulated through the commercial finite element software COMSOL Multiphysics. The results are then compared with those obtained when the inner perforated region is replaced by an equivalent homogenous plate, whose properties are obtained through the asymptotic homogenization technique.

With reference to the colours used in Figure 2a, in the following example, the backplate is constrained as follows: the normal rotation is fixed equal to zero on the whole exterior boundary; the black portion of the boundary is fixed; the green portion of the boundary can only slide in the horizontal direction; the red portion of the boundary is subjected to an inward horizontal imposed displacement $\overline{u}$, bringing the backplate in compression.

3.2.1 Linear buckling analysis

As a first example, we perform a linear buckling analysis of the backplate to determine the critical value of the imposed displacement $\overline{u}_{cr}$, which defines the condition from which non-trivial equilibrium configuration $w(\mathbf{x}) \neq 0$ arises. The critical value reads $\overline{u}_{cr} = 0.0947$ μm for the holed backplate and $\overline{u}_{cr} = 0.0933$ μm for the homogenized one, showing an error of 1.48%.

Figure 4 shows the comparison between the first buckling mode of the backplate modeled with the real geometry and through homogenization: a good agreement between the two solutions can be observed. It should be noted that this result may not remain true for loading conditions that activate the localized buckling mode of the perforated region, which cannot be captured by the homogenization procedure.

3.2.2 Nonlinear static analysis

With reference to the application in MEMS microphones, we consider a nonlinear numerical simulation of the backplate. Initially, a constant pressure $p = 10$ kPa is applied on the blue circular region of radius 260 μm shown in Figure 2a with fixed boundary. Then, keeping constant the applied transversal load, we apply an inward imposed displacement $\overline{u}$, monotonously increasing from 0 to 1 μm. The values chosen for the transversal and membrane load are of the same order of magnitude as those employed in the simulation of the guided free-fall in [10, 11].

The numerical simulation of the model with the real geometry requires 50 minutes, while the homogenized one takes only one minute and a half, showing a reduction of the 97% of the computational time.

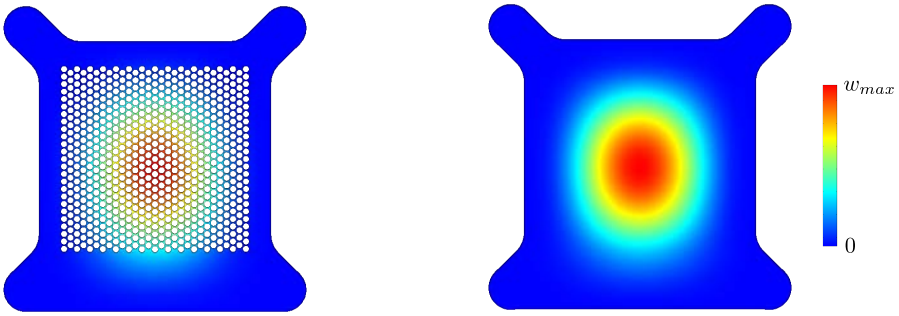

(a) (b)

Figure 4: Contour of the out-plane displacement of the first buckling mode under imposed displacement $\overline{u}$. (a) Real backplate; (b) homogenized model.

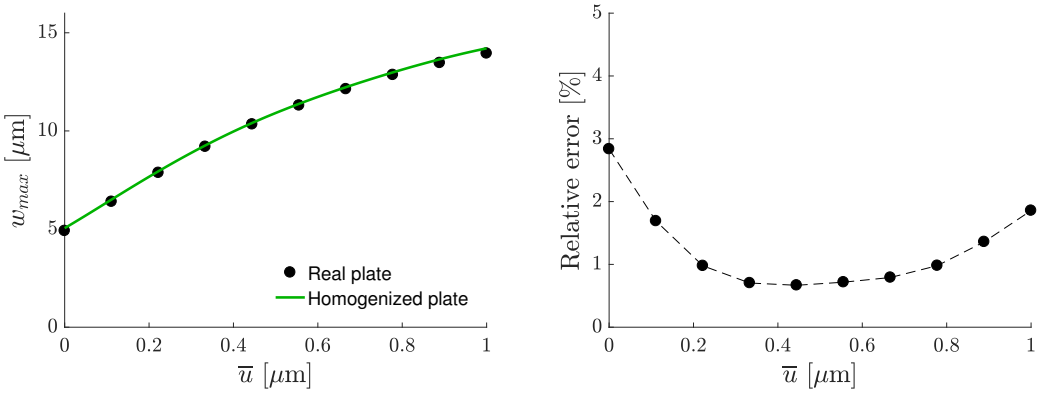

(a) (b)

Figure 5: (a) Maximum deflection of the plate versus imposed displacement for the model with real geometry (markers) and the homogenized one (continuos line); (b) Relative error between real and homogenized solution versus imposed displacement.

Figure 5a shows the maximum out-of-plane displacement of holed backplate (black markers) and the homogenized one (green line) due to monotonously imposed displacement $\overline{u}$. A satisfactory agreement between them is obtained with an error always lower than 3%, see Figure 5b. Due to the nonlinear membrane-flexural coupling of the Föppl-von Kármán theory, the deflection of the plate is magnified as $\overline{u}$ increases. Note that the numerical analysis is performed in the post-buckling phase since $\overline{u}_{cr} \ll 1\ \mu m$.

A good agreement is also obtained in terms of the spatial variation of the plate deflection as shown in Figure 6: the contour of the homogenized displacement well approximates the real one in the whole loading range.

In view of the application in MEMS microphones, one is also interested in the evaluation

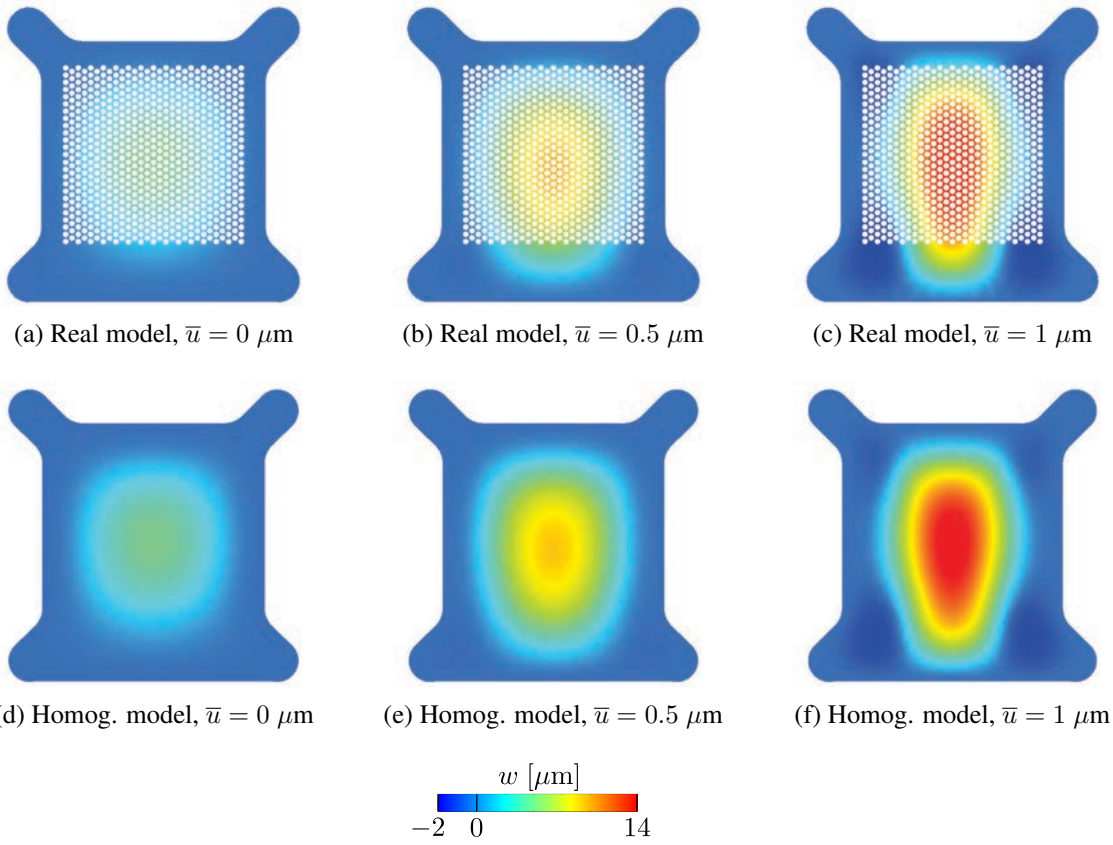

(a) Real model, $\overline{u} = 0$ μm (b) Real model, $\overline{u} = 0.5$ μm (c) Real model, $\overline{u} = 1$ μm

(d) Homog. model, $\overline{u} = 0$ μm (e) Homog. model, $\overline{u} = 0.5$ μm (f) Homog. model, $\overline{u} = 1$ μm

Figure 6: Contour of the out-of-plane displacement for imposed displacements of 0 μm (a,d), 0.5 μm (b,e) and 1 μm (c,f). First row: model with real geometry, second row: homogenized one.

of the stress state in the backplate to assess whether or not the material fails. To this purpose, one has to reconstruct the local fields of the membrane forces and moments starting from the solution of the homogenized plate and using equation (9).

As an example, Figure 7 compares the real distribution of the bending moment M_{11} in the central portion of the perforated backplate for an imposed displacement $\overline{u} = 1$ μm (figure 7a) with that computed in the middle of the homogenized backplate and reconstructed through equation (9) on the unit cell (Figure 7b). A good qualitative agreement between the two distributions is obtained. As expected, a concentration of the bending moment M_{11} is observed in correspondence to the circular holes, in the point indicated with a black circle in Figure 7. The evolution of M_{11} at this point as a function of the imposed displacement $\overline{u}$ is shown in Figure 8a, with black markers for the real backplate and with a continuous line for the homogenized one. The homogenization procedure gives a good estimate, with a maximum error of 8% (see Figure 8b).

The same procedure can be followed to reconstruct the local field of the plate membrane

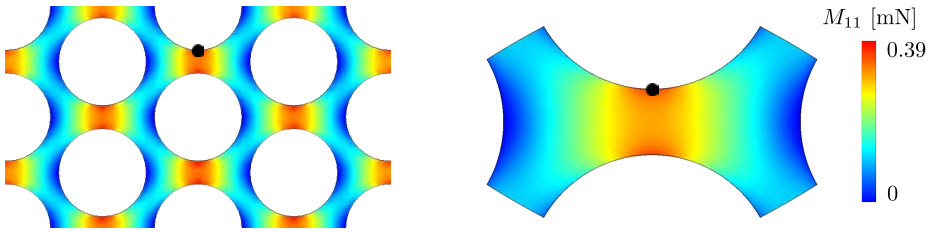

(a) (b)

Figure 7: Contour of the bending moment M_{11} in the case $\overline{u} = 1$ μm. (a) Close-up view of the central region of the real plate; (b) local field in the middle of the homogenized plate.

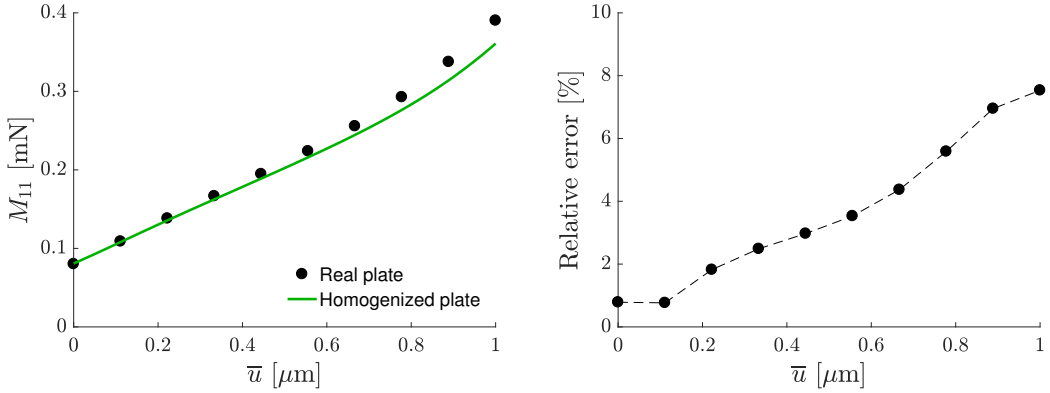

(a) (b)

Figure 8: (a) Evolution of the bending moment M_{11}, as a function of the imposed displacement $\overline{u}$, at the point marked in Figure 7 in the central region of the backplate; (b) relative error between the real bending moment and those obtained through homogenization.

forces, as shown in Figure 9a for the internal force N_{11}, evaluated at the black point depicted in Figure 7. Initially, due to the applied transversal load, the plate is stretched in the x_1-direction, showing a positive value of N_{11}. As the right edge is displaced inward, the plate undergoes compression and N_{11} monotonously decreases and changes sign for $\overline{u} \simeq 0.4$ μm. A good agreement between the homogenized (continuous) and the real (markers) backplate can be observed, as shown by their difference in Figure 9b.

4 CONCLUSIONS

In this work, we apply asymptotic homogenization to the nonlinear plate model proposed by Föppl and von Kármán. This allows us to study the effective behaviour of a periodically perforated backplate, which is employed in MEMS microphones and undergoes transversal loads

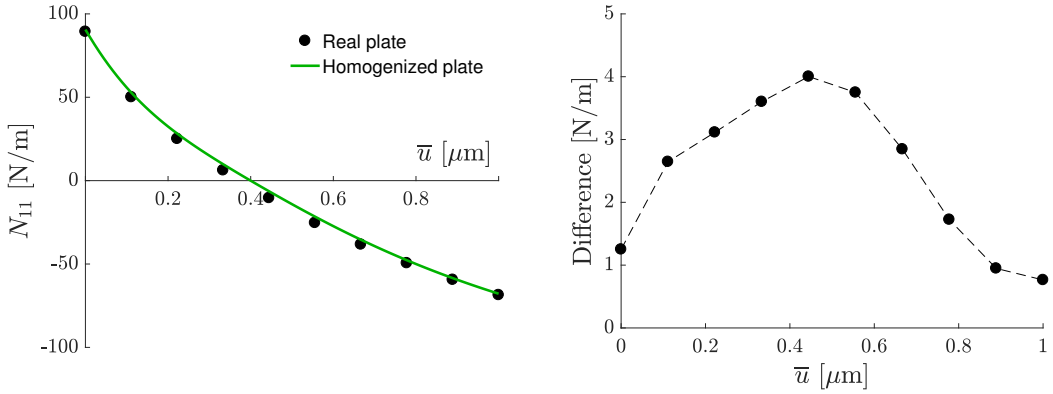

(a) (b)

Figure 9: (a) Evolution of the normal membrane force N_{11}, as a function of the imposed displacement $\overline{u}$, at the point marked in Figure 7 in the central region of the backplate; (b) difference between the real and the homogenized values.

and anchor-imposed displacements. The homogenization procedure allowed us to obtain satisfactory results for nonlinear analyses in the post-buckling regime, both in terms of displacement and local stress state.

Regarding the specific application considered, the next step would be the modelling of the contact between the MEMS membrane with the perforated backplate. As observed by numerical simulation of the real microphone, the region where the membrane touches the backplate involves a large number of cells so qualitatively good results are expected using homogenization also for this loading condition.

REFERENCES

[1] S. Timoshenko and S. Woinowsky-Krieger, *Theory of plates and shells*, 2nd ed. McGraw-Hill, 1959.

[2] A. Bensoussan, J. Lions, and G. Papanicolaou, *Asymptotic Analysis for Periodic Structures*. North- Holland, 1978.

[3] J. L. Auriault, G. Bonnet, I. Nous, and O. Nous, "Dynamique des composites elastiques periodiques," *Arch. Mech.*, vol. 37, no. 4-5, pp. 269–284, 1985.

[4] R. V. Craster, J. Kaplunov, and A. V. Pichugin, "High-frequency homogenization for periodic media High-frequency homogenization," *Proceedings of the Royal Society A: Mathematical, Physical and Engineering Sciences*, 2010.

[5] C. Comi and J. J. Marigo, "Homogenization Approach and Bloch-Floquet Theory for

Band-Gap Prediction in 2D Locally Resonant Metamaterials," *Journal of Elasticity*, vol. 139, pp. 61–90, 2020.

[6] D. Faraci and C. Comi, "Asymptotic homogenization of metamaterials elastic plates," *Journal of Physics: Conference Series*, vol. 2015, no. 012038, 2021.

[7] D. Faraci, C. Comi, and J. J. Marigo, "Band Gaps in Metamaterial Plates: Asymptotic Homogenization and Bloch-Floquet Approaches," *Journal of Elasticity*, vol. 148, 2022.

[8] G. Duvaut, "Homogeneisation des plaques a structure periodique en theorie non lineaire de von Karman," *Lecture Notes in Mathematics*, vol. 665, pp. 55–69, 1978.

[9] T. Lewiński and J. J. Telega, *Plates, Laminates and Shells: Asymptotic Analysis and Homogenization*. World Scientific Publishing, 1999.

[10] D. Faraci, A. Ghisi, S. Adorno, and A. Corigliano, "Top-down , multi-scale numerical simulation of MEMS microphones under guided free fall tests," *Microelectronics Reliability*, vol. 121, p. 114129, 2021.

[11] A. Ghisi, D. Faraci, S. Adorno, and A. Corigliano, "The role of anchor imposed motion in the failure of MEMS microphones under free fall tests," *Microelectronics Reliability*, vol. 135, 2022.